Title

Reduced perfusion in normal-appearing white matter in mild to moderate hypertension as revealed by 3D pseudocontinuous arterial spin labeling

Journal

Journal of Magnetic Resonance Imaging, 43(3)

ISSN

1053-1807

Authors

Wang, Ting
Li, Yanhua
Guo, Xinhong
et al.

Publication Date

2016-03-01

DOI

10.1002/jmri.25023

Peer reviewed

Reduced Perfusion in Normal-Appearing White Matter in Mild to Moderate Hypertension as Revealed by 3D Pseudocontinuous Arterial Spin Labeling

Ting Wang, MD,[1] Yanhua Li, PhD,[2] Xinhong Guo, PhD,[2] Diandian Huang, MD,[1] Lin Ma, PhD,[1] Danny J.J. Wang, PhD,[3] and Xin Lou, PhD[1]*

Purpose: To investigate the hemodynamic changes of normal-appearing white matter (NAWM) in hypertension using the 3D pseudocontinuous arterial spin labeling (pCASL) technique.

Materials and Methods: Seventy-three subjects, including a patient group ($n = 41$; 30 males; age = 47.7 ± 8.3 years; test-time blood pressure [BP] = 155 ± 23/98 ± 11 mmHg) and an age-matched control group ($n = 32$; 14 males; age = 46 ± 8.3 years; test-time BP = 117 ± 8/76 ± 10 mmHg), were recruited and scanned on a 3.0T magnetic resonance imaging (MRI) system using routine MRI sequences and 3D pCASL sequence. The routine MRI sequences were used to further define the NAWM. The cerebral blood flow (CBF) values in various regions of interest (ROIs) were extracted. One-way analysis of variance (ANOVA) and unpaired *t*-test were performed to evaluate the significance of the intergroup difference in CBF modifications.

Results: Compared to healthy volunteers, CBF values in global gray matter (GM) and various NAWM regions were found to be lower ($P < 0.05$) in hypertensive patients, except for genu of corpus callosum (CC), cingulate gyrus, amygdala, pallidum, putamen, and thalamus ($P > 0.05$). Furthermore, compared to the control group, mild hypertension showed significantly reduced CBF in various ROIs ($P < 0.05$), but no intergroup differences in GM, R anterior horn of periventricular WM, and genu of CC ($P > 0.05$), while moderate hypertension showed reduced CBF in all ROIs ($P < 0.05$). However, it was observed that, between mild and moderate hypertensive patients, there were no statistically significant difference in CBF values except for genu of CC ($P < 0.05$).

Conclusion: 3D pCASL has the ability to detect subtle hemodynamic abnormalities in NAWM regions at relatively early stages of hypertension. The observed decreases in CBF in these regions may suggest an increased risk of cerebral small vessel diseases.

J. MAGN. RESON. IMAGING 2016;43:635–643.

White matter (WM) diseases, including WM hyperintensities, lacunars infarcts, cerebral microbleeds,[1] and dilation of perivascular spaces,[2] are commonly observed in cerebral small vessel disease (CSVD) secondary to hypertension. Recent evidence suggests that high blood pressure (BP) can aggravate the cardiovascular burden[3] and result in small vessel structural modifications[4] and impaired blood–brain barrier.[5] Such a loss of vascular integrity may be associated with a decrease in cerebral blood flow (CBF).[6] Previous studies suggest that WM may be especially susceptible to declining perfusion due to its watershed location.[7] Additional studies have further demonstrated that hypertensive subjects with WM diseases may be associated with an increased risk of stroke and cognitive dysfunctions.[8] However, the pathogenesis of WM diseases have not been fully understood, as such an improved characterization of regional decline of CBF in the WM may provide a sensitive measure to better understand the mechanism of subsequent WM diseases.

View this article online at wileyonlinelibrary.com. DOI: 10.1002/jmri.25023

Received May 22, 2015, Accepted for publication Jul 20, 2015.

*Address reprint requests to: X.L., Department of Radiology, Chinese People's Liberation Army (PLA) General Hospital, 28 Fuxing Road, Beijing 100853, China. E-mail: louxin301@gmail.com

The first two authors contributed equally to this work.

From the [1]Department of Radiology, Chinese PLA General Hospital, Beijing, China; [2]Department of Cardiology, Chinese PLA General Hospital, Beijing, China; and [3]Department of Neurology, Department of Radiology, UCLA, Los Angeles, California, USA

Several methods can be used to detect changes in CBF in vivo; for instance, transcranial Doppler technique (TCD),[9] computed tomography (CT) perfusion imaging,[10] positron emission tomography (PET),[11] and magnetic resonance imaging (MRI) including dynamic susceptibility contrast (DSC),[12] and arterial spin labeling (ASL) perfusion imaging. More recently, 3D pseudocontinuous arterial spin labeling (pCASL) using fast spin-echo (FSE) spiral acquisition has been developed to allow higher signal-to-noise ratio (SNR) and better immunity to the arterial transit effect.[13]

The noninvasive nature of 3D pCASL makes it an appealing technique for follow-up examinations of cerebral perfusion in both clinical applications and research studies. However, the reported blood flow in WM was 1.6–4.6-fold lower compared to that in the gray matter (GM).[14] The inherently low flow within the WM and prolonged arterial transit time may confound the perfusion quantification in WM using ASL. Encouragingly, Wu et al[15] have recently showed that pCASL was able to measure perfusion in majority of the cerebral WM at an adequate SNR level by using appropriate tagging duration (2000 msec) and post-labeling delay (PLD) (1500–1800 msec), and noted that further extension of PLD may be needed when prolonged transit time is expected, for example, in the elderly population and patients with ischemia. Similar findings were reported by other groups as demonstrated recently by Wright et al[16] and Li et al.[17]

In the present study, 3D pCASL technique was performed to measure the regional CBF values of normal-appearing white matter (NAWM) and various GM to detect the blood flow differences between hypertensive patients and controls further to investigate the potential hemodynamic changes in hypertension.

Materials and Methods

Ethics Statement

All study protocols were conducted within the guidelines approved by the Institutional Review Board of our hospital. Written informed consent was obtained from each participant.

Patients

Seventy-three subjects with normal cognition, including a hypertensive group ($n = 41$; 30 males; age = 47.7 ± 8.3 years; test-time BP = 155 ± 23/98 ± 11 mmHg) and a control group ($n = 32$; 14 males; age = 46 ± 8.3 years; test-time BP = 117 ± 8/76 ± 10 mmHg), were matched for age distribution and sex, and were pre-screened by referring cardiologists in our hospital. The patients with hypertension had no other diseases combined. The control group consisted of health persons without any diseases. The duration of the hypertension varied, ranging from 6 months to 36 months. The main reference standard for recruiting was based on the classification of hypertension. Further, the hypertensive group consisted of a mild subgroup ($n = 14$; 7 males) and moderate subgroup ($n = 27$; 23 males). The classification of hypertension was defined base on the guideline of European Society of Hypertension (ESH) and European Society of Cardiology (ESC) of 2013. The classification of mild (Stage 1) and moderate hypertension (Stage 2) was based on the average value of awake 24-hour ambulatory BP[18] prior to examination. All patients were diagnosed with essential hypertension and 33 of them had been treated with antihypertensive medicine prior to the present study. Antihypertensive administration, other known vasoactive medications, and caffeine or tea consumption[19] that could affect the CBF were withheld 24 hours before the experiment.

All subjects underwent a physical and a medical history and examination, including regular blood chemistry, echocardiography, ultrasound of carotid artery, and a routine MR scan of brain (read by two neuroradiologists with more than 10 years of experience: X.L. and L.M.) to avoid confounding effects of other diseases, like severe cardiovascular or cerebrovascular disease (eg, previous stroke, transient ischemic attack, myocardial infarction, abnormal intracranial arteries, etc.). For safety concerns, patients with severe hypertension (systolic pressure >180 mmHg or diastolic pressure >110 mmHg), white coat hypertension, and resistant hypertension were excluded. All subjects underwent MR examinations between 2 to 4 PM on the day of scanning.

BP Measurements

Arterial blood oxygen saturation (SPO_2), BP, and heart rate were monitored during all MRI scanning, and were recorded four times (ie, prior to the test, prior to 3D IR-prepared T_1-weighted images [T_1W], pre- and post-3D pCASL sequence) to control for patient conditions.

MRI Protocol

All subjects underwent brain MR exams with routine clinical sequences including axial T_1W, T_2 FLAIR, diffusion-weighted imaging (DWI), and MRA on a 3.0T MR system (Discovery MR750, GE Healthcare, Milwaukee, WI) equipped with an 8-channel head coil to receive signals.

Perfusion-weighted images were obtained using a 3D pCASL technique.[20] In addition to the background suppression pulses within the slab, inferior saturation pulses were applied to suppress the inflowing arterial blood spins. All pCASL images were acquired using a 3D spiral FSE sequence, with the following parameters: 512 sampling points on eight spiral arms, spatial resolution = 3.64 mm, TR = 4844 msec (PLD = 2.0 sec), TE = 10.5 msec, bandwidth = ±62.5 kHz, slice thickness = 4.0 mm, number of slices = 36, labeling duration = 2025 msec, acquisition time = 4:41 minutes, field of view (FOV) = 240 × 240 mm, and number of excitations (NEX) = 3.

In addition to the 3D pCASL images, a high-resolution volumetric T_1W sequence was used to acquire anatomical images with the following parameters: TR = 7.1 msec, TE = 3.1 msec, bandwidth = ±31.2 kHz, TI = 450 msec, slice thickness = 1 mm, number of slices = 360, acquisition time = 4:43 minutes, FOV = 240 × 240 mm, matrix = 256 × 256, and NEX = 1.

Postprocessing

Perfusion maps were generated by pairwise subtraction using the software (Functool 9) onboard the GE MRI scanner (AW4.5, GE

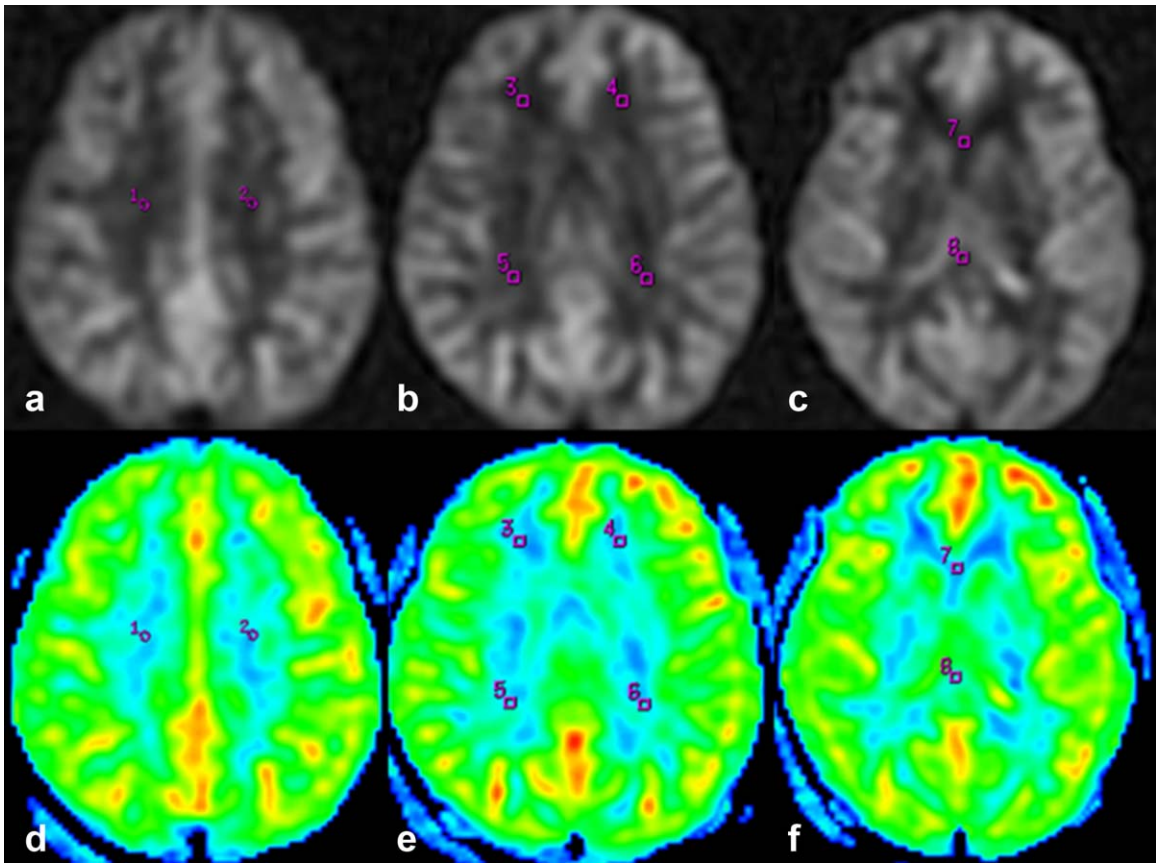

FIGURE 1: Eight ROIs of the NAWM. Round ROIs were placed in eight regions of NAWM in a symmetric fashion on 3D ASL raw data images (a–c) and CBF images (d–f). 1 and 2 indicate ROIs in the R and L centrum semiovale; 3 and 4 in the R and L anterior horns of periventricular WM; 5 and 6 in the R and L posterior horns of periventricular WM; 7 and 8 in the genu and splenium of CC. R = right; L = left.

Healthcare). Subsequent quantifications were performed according to the following equation:

$$CBF = \frac{\lambda\left(1-e^{\frac{-t_{sat}}{T_{1g}}}\right)}{2\alpha T_{1b}\left(1-e^{\frac{-\tau}{T_{1b}}}\right)}\frac{PW}{PD}e^{-\frac{-PLD}{T_{1b}}}$$

where T_{1b} stands for the T_1 of the blood (1600 msec), T_{1g} represents the T_1 of the gray matter (1200 msec), α refers to the labeling efficiency (0.8), λ as the cortex–blood partition coefficient (0.9), t_{sat} as the time of saturation performed before imaging (2000 msec), τ as the labeling duration (2025 msec), and PLD as the postlabeling delay time.

The 3D IR-prepared T_1W images were registered to a standardized space (Montreal Neurological Institute template, MNI space) using the Statistical Parametric Mapping (SPM8) on MatLab 12b (MathWorks, Natick, MA). All quantitative CBF maps were normalized to the MNI space. Standard anatomical regions of interests (ROIs) from WFU Pickatlas (Wake Forest University) were identified. A predefined set of standard ROIs, including the global GM, cingulate gyrus, amygdala, pallidum, putamen, and thalamus, were used to carry out the perfusion analysis in Talairach space.[21,22] The MRI sequences of axial T_1W, T_2 FLAIR, and DWI were analyzed by two neuroradiologists with more than 10 years of experience (X.L. and L.M.) to further define the NAWM. The differences between the two observers were solved by consensus. In addition, eight deep WM were manually drawn to avoid GM-WM contamination.[23] This was done by selecting ROIs at the bilateral centrum semiovale, anterior and posterior horns of periventricular WM, genu and splenium of corpus callosum (CC), in a symmetric fashion on pCASL images (Fig. 1). Moreover, ROIs were obtained from NAWM in patients. CBF values of individual regions of manually drawing WM were assessed between patients and healthy controls. To remove intraobserver variabilities, the ROIs were measured by the one observer (2 years of experience [T.W.] with a coauthor [X.L.] to guide the measurement), but with a second set of measurements performed 4 weeks later. The mean CBF values from all ROIs were estimated and compared.

Statistical Analysis

The averaged CBF values of these two measurements were used for subsequent statistical tests. The intraobserver CBF values of regional WM were evaluated with the intraclass correlation coefficient (ICC). The ICC measured the contribution of the intersubject variances to the total variance, typically ranging from 0–1. ICC values close to 1 indicate high reliability.

All statistical analyses were conducted using the Statistical Program for Social Sciences (SPSS) statistical software (v. 18, Chicago, IL). All the variables exhibited homogeneous variance. A Kolmogorov–Smirnov test was applied to estimate the normality of all

TABLE 1. Baseline Data of the Control and Hypertensive Groups

	Control group (32) Mean ± SD	Hypertensive group (41) Mean ± SD	Units
Age	46 ± 8.4	47.9 ± 8.3	year(s)
Sex, male	32, 14	41, 30	person(s)
Weight	63 ± 8.9	76 ± 15.5	kilograms
SBP	117 ± 7.9	155 ± 20.8	mmHg
DBP	76 ± 10	98 ± 11	mmHg
Heart rate	72 ± 11	76 ± 13	b/min
SPO2	95 ± 4	94 ± 5	percentage
Smoking history	32, 2	41, 17	person(s)
Using aspirin previously	32, 0	41, 27	person(s)
Use of any antihypertensive previously	32, 0	41, 33	person(s)
ACEI or ARB	32, 0	41, 21	person(s)
β-blocker	32, 0	41, 4	person(s)
Calcium channel blocker	32, 0	41, 15	person(s)
Diuretic	32, 0	41, 4	person(s)

SBP = systolic blood pressure; DBP = diastolic blood pressure; ACEI = angiotensin converting enzyme inhibitors; ARB = angiotensin receptor blocker.

the measured parameters. Levine's test was performed to compare the intergroup difference in the homogeneity of the variance. One-way analysis of variance (ANOVA) and unpaired *t*-tests were performed to compare the CBF significance of the normally distributed variables between the groups. $P < 0.05$ was regarded as the statistical significance threshold in the present study.

Results

The baseline values of the control and hypertensive groups were reported in Table 1, which include subjects' demographic and physiological data. Among these subjects, the CBF values were observed to be lower in hypertensive patients than those in the normotensive subjects, specifically, in the global GM (51.37 ± 8.1 vs. 45.71 ± 8.32, $P = 0.005$), centrum semiovale (R: 25.45 ± 3.45 vs. 21.16 ± 4.82, $P = 0.000$; L: 25.87 ± 3.69 vs. 21.99 ± 3.8, $P = 0.000$), anterior horns of periventricular WM (R: 23.09 ± 3.99 vs. 19.92 ± 3.748, $P = 0.002$; L: 23.97 ± 4.34 vs. 20.3 ± 3.765, $P = 0.001$), posterior horns of periventricular WM (R: 27.9 ± 4.46 vs. 22.37 ± 4.81, $P = 0.000$; L: 26.84 ± 5.1 vs. 21.89 ± 3.63, $P = 0.000$), and

TABLE 2. Mean CBF Values and Standard Deviation (SD) in Various GM ROIs for the Control and Hypertensive Groups

ROIs	Control group		Hypertensive group		*P* value	Mean difference
	Mean	SD	Mean	SD		
Cingulate gyrus	46.72	7.791	43.61	6.854	0.076	3.114
Amygdala	41.71	6.749	39.61	6.134	0.172	2.099
Pallidum	37.34	5.983	36.17	5.359	0.382	1.176
Putamen	40.96	6.216	39.89	5.996	0.464	1.065
Thalamus	48.75	7.91	45.5	8.52	0.102	3.245

Perfusion was measured in units of mL/100 cc gray matter/min.
Compared to the normal subjects, CBF values in various GM implicated no significant fluctuation.

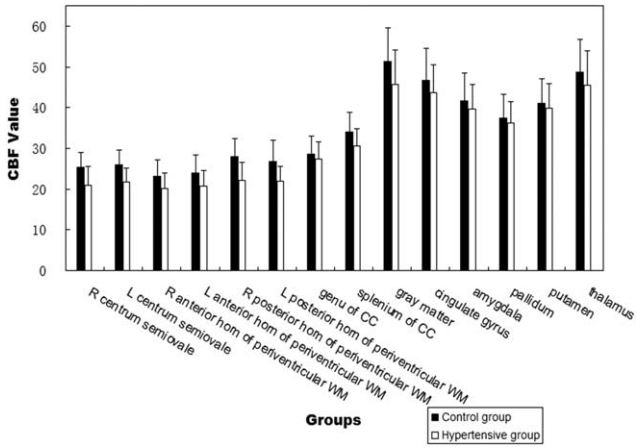

FIGURE 2: Bar chart with the standard deviation (SD) for the CBF of the control and hypertensive groups in the regional ROIs. Compared with the control group, the hypertensive group exhibited decreased CBF, and the SD was below the acceptable wave range. Perfusion was measured in units of mL/100 cc gray matter/min.

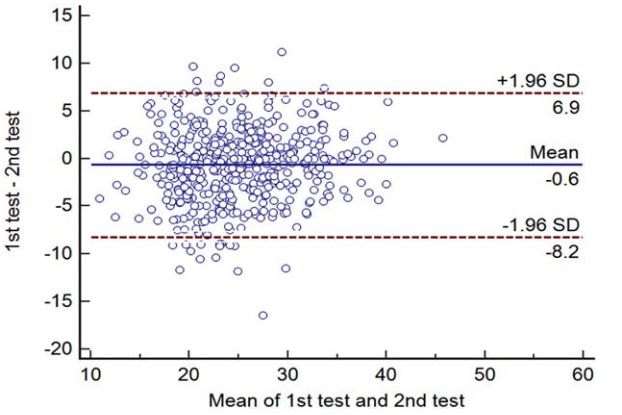

FIGURE 3: Bland–Altman plots together with the 95% CI. Bland–Altman plots of two times CBF measurements form eight WM ROIs in all subjects. Perfusion was measured in units of mL/100 cc gray matter/min.

splenium of CC (34 ± 4.86 vs. 30.4 ± 4.28, $P = 0.003$). However, distinct from other ROIs, the CBF values in the genu of CC, cingulate gyrus, amygdala, pallidum, putamen, and thalamus demonstrated no statistically significant ($P > 0.05$) intergroup difference (Tables 2, 4, Fig. 2). As shown in Table 3 and Fig. 3, the intraobserver variability of manually drawing WM was relatively small, with ICC ranging from 0.708 to 0.911. Furthermore, compared to the control group, mild hypertensive patients showed significantly reduced CBF in the centrum semiovale (R: 25.45 ± 3.447 vs. 25.76 ± 5.708, $P = 0.011$; L: 25.87 ± 3.69 vs. 22.71 ± 3.647, $P = 0.011$), L anterior horn of periventricular WM (23.97 ± 4.34 vs. 21.22 ± 3.769, $P = 0.048$), posterior horns of periventricular WM (R: 27.9 ± 4.463 vs. 23.04 ± 4.738, $P = 0.002$; L: 26.84 ± 5.101 vs. 22.77 ± 3.459, $P = 0.01$) and splenium of CC (34.01 ± 4.856 vs. 30.49 ± 3.779, $P = 0.021$), but no significant intergroup differences in GM, R anterior horn of periventricular WM, and genu of CC ($P > 0.05$), while moderate hypertensive patients showed significantly reduced CBF in all ROIs ($P < 0.05$) (Table 4, Fig. 4). However, it was observed that between the mild and moderate hypertensive patients, there were no statistically significant difference in CBF values other than that in the genu of CC (29.27 ± 2.838 vs. 26.23 ± 4.577, $P = 0.014$) (Table 4, Fig. 4).

Discussion

WM in the brain is a particularly relevant and potentially indicative area of CSVD in hypertensive patients. However, based on the hypothesis we raised in this study that, at the early stage of hypertension, most of the WM regions can be normal-appearing despite their potentially reduced perfusion level. Recent progress in MRI perfusion techniques open the

TABLE 3. Intraclass Correlation Coefficient (ICC) Values and 95% Confidence Interval (CI) for Intraobserver Variability

ROIs	ICC	95% CI
R centrum semiovale	0.843	0.738-0.906
L centrum semiovale	0.782	0.635-0.870
R anterior horn of periventricular WM	0.730	0.549-0.839
L anterior horn of periventricular WM	0.708	0.511-0.826
R posterior horn of periventricular WM	0.858	0.762-0.915
L posterior horn of periventricular WM	0.854	0.755-0.913
genu of CC	0.871	0.784-0.923
splenium of CC	0.911	0.851-0.947

The intraobserver variability was insignificant, with ICC ranging from 0.708 to 0.911.
CC = corpus callosum; WM = white matter

TABLE 4. Mean CBF Values and Standard Deviation (SD) in Various ROIs for Control Group, Hypertensive Group, Mild and Moderate Hypertensive Group

ROIs	Con G		Hp G		Mil Hp		Mod Hp		*P* value			
	Mean	SD	Mean	SD	Mean	SD	Mean	SD	Con G vs. Hp G	Con G vs. Mil Hp	Con G vs. Mod Hp	Mil Hp vs. Mod Hp
GM	51.37	8.099	45.71	8.323	48.06	8.947	44.44	7.853	0.005	0.223	0.002	0.193
1	25.45	3.447	20.94	4.517	21.76	5.708	20.5	3.783	0.000	0.011	0.000	0.407
2	25.87	3.69	21.71	3.349	22.71	3.647	21.17	3.118	0.000	0.011	0.000	0.169
3	23.09	3.987	20.08	3.948	21.39	5.269	19.37	2.896	0.002	0.242	0.000	0.200
4	23.97	4.34	20.63	3.876	21.22	3.769	20.31	3.97	0.001	0.048	0.002	0.488
5	27.9	4.463	22.12	4.352	23.04	4.738	21.63	4.141	0.000	0.002	0.000	0.335
6	26.84	5.101	21.89	3.625	22.77	3.459	21.42	3.698	0.000	0.01	0.000	0.265
7	28.64	4.345	27.3	4.275	29.27	2.838	26.23	4.577	0.200	0.624	0.048	0.014
8	34.01	4.856	30.54	4.29	30.49	3.779	30.57	4.613	0.002	0.021	0.009	0.957

Perfusion was measured in units of mL/100 cc gray matter/min
GM = gray matter; 1 = R centrum semiovale; 2 = L centrum semiovale; 3 = R anterior horn of periventricular WM; 4 = L anterior horn of periventricular WM; 5 = R posterior horn of periventricular WM; 6 = L posterior horn of periventricular WM; 7 = genu of CC; 8 = splenium of CC; Con G = Control group; Hp G = Hypertensive group; Mil Hp = Mild hypertensive group; Mod Hp = Moderate hypertensive group.

possibility to noninvasively study the CBF, which could shed light on the potential effect of hypertension on perfusion in the WM, and in turn provide an early imaging biomarker to assess the risk of CSVD.

Recent studies have demonstrated that WM diseases tend to cluster in several specific locations: the deep WM of the centrum semiovale, the anterior and posterior horns of the periventricular region, and the genu and splenium of

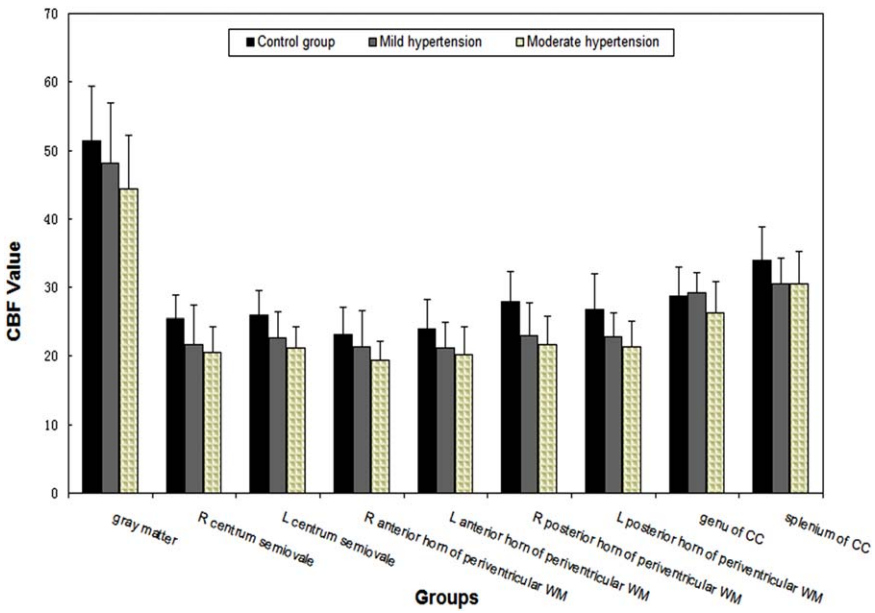

FIGURE 4: Bar chart with the standard deviation (SD) for the CBF of the control group, mild and moderate hypertension in the regional ROIs. Compared to the control group, mild hypertension exhibited declined CBF in most ROIs, while a slight fluctuation in GM, R anterior horn of periventricular WM, and genu of CC, and moderate hypertension exhibited declined CBF in all of ROIs; furthermore, CBF values suggested no significant fluctuation between mild and moderate hypertension in most of the ROIs except for the genu of CC, and the SD was below the acceptable wave range. Perfusion was measured in units of mL/100 cc gray matter/min.

the CC.[24–26] In general, WM receives most of its blood supply through long penetrating arteries that arise from the vessels located in the subarachnoid space.[27] These penetrating vessels do not arborize but emit perpendicularly oriented distributing vessels that irrigate the WM, each of which provide and guarantee the blood supply to a cylindrically shaped metabolic unit.[28] Furthermore, the anastomoses between these vessels are relatively scarce. Given this unique pattern of vascularization, the deep WM (ie, centrum semiovale and periventricular WM) is considered an arterial border zone (or watershed), which is particularly susceptible of being injured by systemic or focal declining in CBF[7] in hypertension. The microcirculation of CBF supplies brain tissues with sufficient nutrients and removes metabolic waste; hence, a decreased CBF can lead to ischemic stroke or cerebrovascular complications, such as leukoaraiosis and even vascular cognitive impairment in hypertension. However, the pathogenesis of WM hemodynamic changes and subsequent cerebrovascular complications remains unclear.

In our study, it was found that the CBF in hypertensive subjects was reduced globally in the GM, as well as all regions of NAWM except for the genu of CC. In comparison, the cingulate gyrus, thalamus, and basal ganglia region (amygdala, pallidum, putamen) did not exhibit statistically significant changes in hypertension. Based on these findings, we propose the following inferences. First, it appeared that the cortical GM was sufficiently perfused in the presence of ischemic injury in patients with no cognitive dysfunction, likely due to its abundant collateral circulation. Second, it was demonstrated that hypoperfusion was clustered in regions of NAWM, where hypertensive patients most frequently develop leukoaraiosis over time. Third, there was no detectable CBF changes in areas included cingulate gyrus, thalamus, and basal ganglia. As a component of the limbic system, the cingulate gyrus has relatively small variation during the development of the brain. It possesses a relatively stable CBF, likely related to the direct perfusion of the main branch of the anterior cerebral artery, and can be used as a baseline perfusion of hypertension. The CBF of the cingulate gyrus was only reported to decline at later stages of neurodegeneration.[29] Our result endorses this finding, showing a slight CBF fluctuation in the cingulate gyrus. Moreover, the deep GM nuclei such as thalamus and basal ganglia were chosen as a reference of deep WM, and the mild CBF fluctuation was probably because these areas were directly perfused by the main branch of the basilar artery and middle cerebral artery (ie, lenticulostriate artery).

It is generally known that CSVD secondary to hypertension is the leading cause of WM diseases.[28] As a basal requirement for normal function, the brain acquires a disproportionally large amount of blood flow and possesses a complex cerebral autoregulation system to maintain a constant CBF across a range of BPs. However, prolonged chronic hypertension can lead to alterations in small vessels, including atherosclerosis of the smaller (100–500 μm) perforating arteries and the arteriolosclerosis of the smaller (<100 μm) vessels.[30] These small arteries and arterioles undergo medial thickening associated with hyaline deposition and intimal proliferation, which accounts for the reduction in luminal diameter and an increased resistance to the flow.[28] As arterial narrowing increases, it results in a reduction in capillary perfusion, which can further lead to ischemia and lacunar infarction.[31] Furthermore, attributable to the inability of sclerotic vessels to dilate, occasional drops in BP can lead to a significant decrease in blood flow into the WM among patients with arteriolosclerotic vessels.[32] Previous studies have demonstrated that autoregulatory limits were shifted upwards among hypertensive subjects[33]; hence, a rapid reduction of blood pressure, even within physiological limits, could result in a marked reduction (or worse, ischemia) in the WM perfusion among chronically hypertensive patients, consequently lead to ischemia, stroke, and cognitive dysfunction. Thus, our finding of decreased CBF in hypertension may indicate a potentially flow-related mechanism in the pathogenesis of leukoaraiosis, instead of blood–brain barrier dysfunction with increased capillary permeability.[34]

We also observed that CBF in genu of CC declined in moderate hypertension compared with both the control group and mild hypertension, whereas the CBF demonstrated no obvious fluctuation between mild hypertension and the control group, while the CBF in splenium of CC declined in both total hypertensive subjects, mild and moderate hypertension compared with the control group, but no significant difference between mild and moderate hypertension, likely attributed to the blood supply of CC. A previous study has described the vascular supply of the CC[35] in detail. The subcallosal and medial callosal arteries, branches of the anterior communicating artery, provide the main supply for the anterior portion of the CC. The posterior pericallosal artery, a branch of the posterior cerebral artery, supplies the splenium, disposing them to generalized atherosclerosis. Leading to that, the splenium of the CC was affected more often than the body and genu. Consistent with the previous study, this finding indicated that the CBF in genu of the CC was relatively stable, that only to moderate hypertension can exhibit declined CBF, and meanwhile the decline in mild hypertension was not obviously, comparing the control group with the hypertensive subjects, mixing mild and moderate hypertension, weaken the difference between subhypertensive groups, resulting in that there was no significant difference between the control and hypertensive groups but a significant difference between the control and moderate hypertensive groups. In addition, the splenium of CC was susceptible of being injured by declined CBF in hypertension and exhibited declining of CBF in

mild hypertension; therefore, secondary injury based on the previous injury in moderate hypertension may not demonstrate a significant difference compared to mild hypertension.

We note two potential limitations in our study. First, our sample size was relatively small, which may account for the inability to reach statistical significance in the genu of CC (the 95% confidence interval for mean was 27.02–30.23 vs. 25.93–28.76). Second, the scan-time BP only reflected the temporary BP rather than the necessary tendency of BP variabilities. Moreover, the CBF response to orthostatic challenge or the 24-hour ambulatory systolic BP was not investigated, which were previously recorded in the clinical history.

We conclude that 3D pCASL has the ability to detect subtle WM hemodynamic abnormalities even at the early stage of hypertension, even when these WM regions appear normal in conventional MR images. Furthermore, the observed reduction in CBF clusters in several specific WM regions of hypertensive subjects, indicating a potential risk of cerebral small vessel complications, and as a result it could serve as an early imaging marker of hypertension-related CSVD.

Acknowledgments

Contract grant sponsor: National Natural Science Foundation of China; contract grant number: 81101034 (to X.L.).
We thank Bensheng Qiu, PhD, and Xiaoxuan He, MD, at Department of Electronic Science and Technology, University of Science and Technology of China, and Zhenyu Zhou, PhD, Bing Wu, PhD, and Dandan Zhen, PhD, at GE Healthcare, Beijing, China, for excellent technical assistance.

References

1. Klarenbeek P, van Oostenbrugge RJ, Rouhl RP, Knottnerus IL, Staals J. Ambulatory blood pressure in patients with lacunar stroke: association with total MRI burden of cerebral small vessel disease. Stroke 2013;44:2995–2999.
2. Martinez-Ramirez S, Pontes-Neto OM, Dumas AP, et al. Topography of dilated perivascular spaces in subjects from a memory clinic cohort. Neurology 2013;80:1551–1556.
3. Black HR. The burden of cardiovascular disease: following the link from hypertension to myocardial infarction and heart failure. Am J Hypertens 2003;16:4S–6S.
4. Kashgarian M. Pathology of small blood vessel disease in hypertension. Am J Kidney Dis 1985;5:A104–A110.
5. Tang JP, Xu ZQ, Douglas FL, Rakhit A, Melethil S. Increased blood-brain barrier permeability of amino acids in chronic hypertension. Life Sci 1993;53:PL417–PL420.
6. Cohen RA. Hypertension and cerebral blood flow: implications for the development of vascular cognitive impairment in the elderly. Stroke 2007;38:1715–1717.
7. Jokinen H, Lipsanen J, Schmidt R, et al. Brain atrophy accelerates cognitive decline in cerebral small vessel disease: the LADIS study. Neurology 2012;78:1785–1792.
8. Messerli FH, Williams B, Ritz E. Essential hypertension. Lancet 2007; 370:591–603.
9. Zhang R, Witkowski S, Fu Q, Claassen JA, Levine BD. Cerebral hemodynamics after short- and long-term reduction in blood pressure in mild and moderate hypertension. Hypertension 2007;49: 1149–1155.
10. Gould B, McCourt R, Asdaghi N, et al. Autoregulation of cerebral blood flow is preserved in primary intracerebral hemorrhage. Stroke 2013;44:1726–1728.
11. Zazulia AR, Videen TO, Morris JC, Powers WJ. Autoregulation of cerebral blood flow to changes in arterial pressure in mild Alzheimer's disease. J Cereb Blood Flow Metab 2010;30:1883–1889.
12. Li G, Shih YY, Kiel JW, De La Garza BH, Du F, Duong TQ. MRI study of cerebral, retinal and choroidal blood flow responses to acute hypertension. Exp Eye Res 2013;112:118–124.
13. Gould B, McCourt R, Asdaghi N, et al. Autoregulation of cerebral blood flow is preserved in primary intracerebral hemorrhage. Stroke 2013;44:1726–1728.
14. van Osch MJ, Teeuwisse WM, van Walderveen MA, Hendrikse J, Kies DA, van Buchem MA. Can arterial spin labeling detect white matter perfusion signal? Magn Reson Med 2009;62:165–173.
15. Wu WC, Lin SC, Wang DJ, Chen KL, Li YD. Measurement of cerebral white matter perfusion using pseudo-continuous arterial spin labeling 3t magnetic resonance imaging — an experimental and theoretical investigation of feasibility. PLoS One 2013;8:e82679.
16. Wright SN, Kochunov P, Chiappelli J, et al. Accelerated white matter aging in schizophrenia: role of white matter blood perfusion. Neurobiol Aging 2014;35:2411–2418.
17. Li X, Sarkar SN, Purdy DE, Briggs RW. Quantifying cerebellum grey matter and white matter perfusion using pulsed arterial spin labeling. Biomed Res Int 2014;2014:108691.
18. Chobanian AV, Bakris GL, Black HR, et al. Seventh report of the Joint National Committee on Prevention, Detection, Evaluation, and Treatment of High Blood Pressure. Hypertension 2003;42:1206–1252.
19. Vidyasagar R, Greyling A, Draijer R, Corfield DR, Parkes LM. The effect of black tea and caffeine on regional cerebral blood flow measured with arterial spin labeling. J Cereb Blood Flow Metab 2013;33: 963–968.
20. Dai W, Garcia D, de Bazelaire C, Alsop DC. Continuous flow-driven inversion for arterial spin labeling using pulsed radio frequency and gradient fields. Magn Reson Med 2008;60:1488–1497.
21. Maldjian JA, Laurienti PJ, Kraft RA, Burdette JH. An automated method for neuroanatomic and cytoarchitectonic atlas-based interrogation of fMRI data sets. Neuroimage 2003;19:1233–1239.
22. Lancaster JL, Woldorff MG, Parsons LM, et al. Automated Talairach atlas labels for functional brain mapping. Hum Brain Mapp 2000;10: 120–131.
23. van Gelderen P, de Zwart JA, Duyn JH. Pittfalls of MRI measurement of white matter perfusion based on arterial spin labeling. Magn Reson Med 2008;59:788–795.
24. DeCarli C, Fletcher E, Ramey V, Harvey D, Jagust WJ. Anatomical mapping of white matter hyperintensities (WMH): exploring the relationships between periventricular WMH, deep WMH, and total WMH burden. Stroke 2005;36:50–55.
25. Sachdev P, Wen W, Chen X, Brodaty H. Progression of white matter hyperintensities in elderly individuals over 3 years. Neurology 2007; 68:214–222.
26. Yoshita M, Fletcher E, Harvey D, et al. Extent and distribution of white matter hyperintensities in normal aging, MCI, and AD. Neurology 2006;67:2192–2198.
27. Kochunov P, Glahn DC, Hong LE, et al. P-selectin expression tracks cerebral atrophy in Mexican-Americans. Front Genet 2012;3:65.

28. Birns J, Markus H, Kalra L. Blood pressure reduction for vascular risk: is there a price to be paid? Stroke 2005;36:1308–1313.

29. Xekardaki A, Rodriguez C, Montandon ML, et al. Arterial spin labeling may contribute to the prediction of cognitive deterioration in healthy elderly individuals. Radiology 2015;274:490–499.

30. Fisher CM. Pathological observations in hypertensive cerebral hemorrhage. J Neuropathol Exp Neurol 1971;30:536–550.

31. Ostrow PT, Miller LL. Pathology of small artery disease. Adv Neurol 1993;62:93–125.

32. Pantoni L, Garcia JH. Cognitive impairment and cellular/vascular changes in the cerebral white matter. Ann N Y Acad Sci 1997;826:92–102.

33. Strandgaard S. Autoregulation of cerebral blood flow in hypertensive patients: the modifying influence of prolonged antihypertensive treatment on the tolerance to acute, drug-induced hypotension. Circulation 1976;53:720–727.

34. Smith EE. Leukoaraiosis and stroke. Stroke 2010;41:S139–S143.

35. Ture U, Yasargil MG, Krisht AF. The arteries of the corpus callosum: a microsurgical anatomic study. Neurosurgery 1996;39:1075–1085.